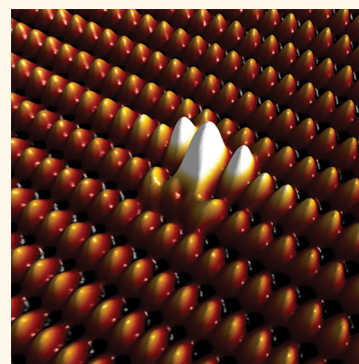


# Site-Dependent Ambipolar Charge States Induced by Group V Atoms in a Silicon Surface

Philipp Studer,<sup>†,‡</sup> Veronika Brázdová,<sup>†,¶</sup> Steven R. Schofield,<sup>†,¶</sup> David R. Bowler,<sup>†,¶</sup> Cyrus F. Hirjibehedin,<sup>†,¶,§</sup> and Neil J. Curson<sup>†,‡,\*</sup>

<sup>†</sup>London Centre for Nanotechnology, <sup>‡</sup>Department of Electronic and Electrical Engineering, <sup>¶</sup>Department of Physics and Astronomy, <sup>§</sup>Department of Chemistry, University College London, London, U.K.

**ABSTRACT** We report that solitary bismuth and antimony atoms, incorporated at Si(111) surfaces, induce either positive or negative charge states depending on the site of the surface reconstruction in which they are located. This is in stark contrast to the hydrogenic donors formed by group V atoms in silicon bulk crystal and therefore has strong implications for the design and fabrication of future highly scaled electronic devices. Using scanning tunnelling microscopy (STM) and density functional theory (DFT) we determine the reconstructions formed by different group V atoms in the Si(111)2 × 1 surface. Based on these reconstructions a model is presented that explains the polarity as well as the location of the observed charges in the surface. Using locally resolved scanning tunnelling spectroscopy we are furthermore able to map out the spatial extent over which a donor atom influences the unoccupied surface and bulk electronic states near the Fermi-level. The results presented here therefore not only show that a dopant atom can induce both positive and negative charges but also reveal the nature of the local electronic structure in the region of the silicon surface where an individual donor atom is present.



**KEYWORDS:** silicon · dopants · STM · DFT · bismuth · antimony

Donor atoms in silicon have demonstrated great potential for the fabrication of atomic-scale devices<sup>1</sup> and the implementation of future computation concepts such as quantum information processing (QIP) and spintronics.<sup>2,3</sup> Whereas initial solid-state QIP proposals were based on the use of a single dopant species (P), more recent ideas take advantage of a combination of different group V donor elements, including heavier donors such as bismuth (Bi).<sup>4–7</sup> Their favorable properties, including large ionization energies and longer spin–lattice relaxation times, allow the facilitation of novel device functionalities at significantly higher operation temperatures. However, this also leads to new challenges as Bi, the largest group V donor with the highest ionization energy, has a very low solubility in silicon. It has been suggested that a vacancy donor complex might form to release strain in the vicinity of the large dopant core,<sup>8,9</sup> potentially altering the characteristics of solitary Bi dopants. This makes investigation into the atomic

scale properties of Bi and other group V donors of significant importance.

When considering the role of group V donors in silicon for future generation devices, it must be remembered that device components will be within a few nanometres of one another. Consequently one must not only consider the properties of donors in the ideal “bulk” lattice but also in an environment where the lattice has undergone some perturbation. An upper bound on the extent to which the lattice can be perturbed is conveniently provided by the crystal surface. Here the structure of the surface is sufficiently distorted from that of the bulk that even the position(s) that a dopant atom might substitute into the lattice, or the coordination that it would have, cannot be assumed *a priori*. In addition the electronic landscape experienced by a dopant is also modified from that of the bulk.

Here we show that the properties of Sb and Bi dopants substituted in the (111)2 × 1 surface of silicon deviate significantly from those properties expected of dopants in

\* Address correspondence to n.curson@ucl.ac.uk.

Received for review August 28, 2012 and accepted November 13, 2012.

Published online November 27, 2012  
10.1021/nn3039484

© 2012 American Chemical Society

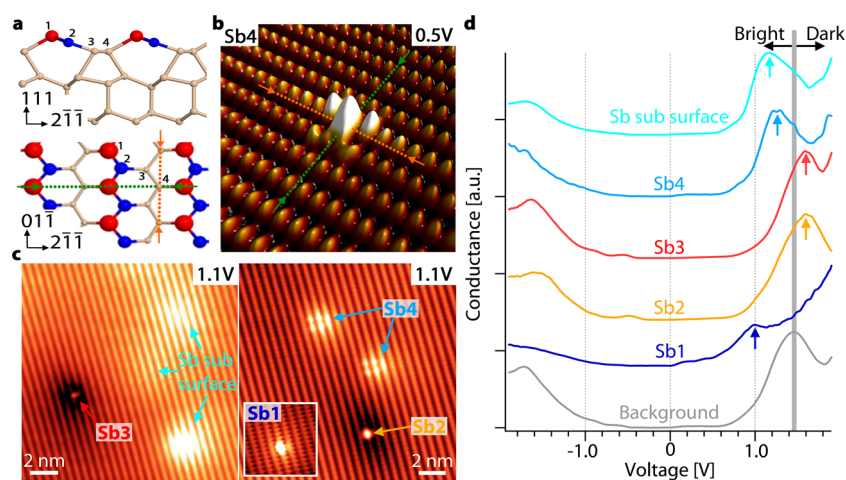


**Figure 1.** (a) Pandey reconstructed Si(111)2 × 1 surface; distinguishable surface sites 1–4 are labeled. The atoms colored red (blue) correspond to the up-buckled (down-buckled) Si atoms of the dimer chain. (b) Empty state topography image of an Sb atom in site 4, as determined by crystal symmetry, indicated by the arrows. (c) Identified features on the Sb doped substrate. (d) STS acquired in the immediate surroundings of the different Sb features. The band shift induced by the charge is clearly visible in the peak around 1.2 V when compared to the background.

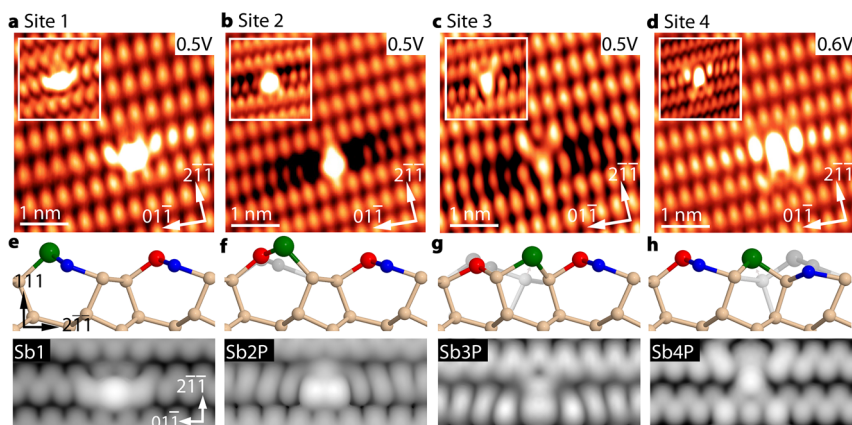


**Figure 2.** (a–d) Empty state topography images of Sb (Bi inset) for surface sites 1–4, respectively. (e–h) (Top) Identified ground state reconstructions with the original Pandey model underlaid in gray, Sb atoms shown enlarged, in green. The atoms colored red (blue) correspond to the up-buckled (down-buckled) Si atoms of the dimer chain. Bottom: Simulated STM images for Sb1 and the "pushed-up" reconstructions Sb2P–Sb4P, calculated to the equivalent of a sample bias voltage of 0.5 V.

the bulk. Using cross-sectional STM and STS in conjunction with DFT, we characterize solitary Sb and Bi atoms at the atomic scale, determining their reconstructions in the silicon surface and showing they exhibit the unexpected property of site-dependent ambipolar charge states. The capability of STS to resolve the local density of states also allows us to map out the spatial extent over which a donor atom influences the unoccupied surface and bulk electronic states near the Fermi-level. This information about how the characteristics of single dopants change if they are placed in a silicon surface provides vital insights for the design and fabrication of future few-dopant devices.

## RESULTS AND DISCUSSION

For the last few decades, charge-based microelectronics have relied on a simple donor model, where group V atoms with a low ionization energy donate their fifth electron to the bulk, engineering the band

structure of silicon. However, as the scaling of devices approaches the single dopant limit, novel architectures require solitary donors to be positioned in close proximity to gates, isolators, and surfaces. These material interfaces represent abrupt changes in the dielectric and structural properties of a semiconductor and we therefore conducted an atomic scale study to reveal how this influences nearby positioned solitary donors.

Cross-sectional STM was used to characterize solitary Sb and Bi atoms in the Si(111)2 × 1 surface. Figure 1a shows the Pandey model of the Si(111)2 × 1 surface reconstruction.<sup>10</sup> To compare atoms of different group V elements in atomically identical environments their exact crystal site, labeled 1–4 in Figure 1a, was determined using crystal symmetry, as indicated by the arrows in Figure 1a,b. On both the Sb and the Bi doped wafers a similar set of five reoccurring, distinctive features was identified, as shown in Figure 1c for Sb and in Figure 2 for Bi. Four of the features could be assigned to

the four distinguishable surface sites, accordingly labeled Sb1–4 in Figure 1c, in excellent agreement with the expected behavior of substitutional group V atoms in a silicon surface. The fifth feature was found to be characterized by only a weak contrast enhancement in empty states, superimposed on the undisturbed atomic corrugation of the Si(111)2 × 1 surface. Such a protrusion is commonly attributed to the charge signature of an ionized subsurface donor as measured in STM.<sup>11</sup>

The most striking observation in Figure 1c is the fact that two of the features show a dark depression around them while the other three are surrounded by a bright protrusion. In STM images, it is well established that brightening or darkening around surface features arises from charging effects that induce local band-bending.<sup>12</sup> The bright protrusion around the subsurface position on sites 1 and 4 is therefore indicating a positive charge, inducing a downward band shift and increasing the accessible electrons for tunnelling in the empty states. The Sb atoms in sites 2 and 3 however show a depression around them, indicating a negative charge that shifts the bands upward. Scanning tunnelling spectroscopy (STS) was used to confirm the charge state of the different features by directly measuring the induced band shift as shown in Figure 1d for Sb; identical results were obtained for Bi. Tip induced band bending is negligible at the surface of highly doped Si(111)2 × 1 surfaces<sup>13</sup> due to the Fermi level pinning in the surface states<sup>14</sup> and does therefore not have to be taken into account. The upward (downward) shift of peaks in the spectra is clearly visible, demonstrating that bands are bent upward (downward) around the different sites and therefore confirming their negative (positive) charge state. This is unexpected as group V atoms in silicon are usually assumed to be either positively charged (ionized) or neutral (not ionized), whereas negative charge states are usually attributed to ionized acceptors.

Site-dependent charging of group V atoms has not previously been observed in silicon, and the fact that we measure both charge polarities using identical tunnelling conditions for spectroscopy suggests that the observed charge states are not tip induced but intrinsically stable. This is further supported by the observation that the charge signatures in STM images were stable over a wide range of bias voltages, from 0.5 to 2.0 V. The mechanism for the formation of the ambipolar, site-dependent charge states must therefore be substantially different compared to previous work where the charging of Si in GaAs or of the P:Si heterodimer in Si(001) was influenced using the STM tip as a gate.<sup>15,16</sup> P in Si(111)2 × 1 showed a positive charge at room temperature<sup>17</sup> and a neutral charge state at 8 K<sup>18</sup> for all crystal sites, which is very different from what we observe for Sb and Bi.

To explain the different charge states, the atomic reconstruction of the Sb and Bi atoms in the different crystal sites of the surface was investigated using

**TABLE 1. Element-Dependent Ground State Energies. Energy Gained by the “Pushed-up” Reconstructions S2P–S4P Compared to the Pandey Reconstructions S2–S4 for All Group V Elements<sup>a</sup>**

element	atomic	ionization	size	S2–S2P	S3–S3P	S4–S4P
	number	energy	[ $\Delta V/V_{Si}$ ]			
phosphorus (P)	15	44 meV	–8%	0.04 eV	0.64 eV	0.33 eV
arsenic (As)	33	54 meV	+4%	0.13 eV	0.76 eV	0.45 eV
antimony (Sb)	51	39 meV	+17%	0.27 eV	0.81 eV	0.44 eV
bismuth (Bi)	83	71 meV	+30%	0.44 eV	1.05 eV	0.75 eV

<sup>a</sup> Indicated are also basic donor element properties, ionization energy, and size measured relative to silicon.<sup>20</sup>

voltage-dependent imaging and DFT, as shown in Figure 2. Surprisingly, DFT simulations for substitutional Sb in sites 2–4 resulted in ground state reconstructions different from the Pandey model, with the dopant pushed upward, as shown in Figure 2f–h. Identical results were found for Bi as shown in Supporting Information, Figure S1. In Figure 2 it can be seen that the new reconstruction of site 2 displays a change of buckling for the Sb atom, whereas the new reconstructions of sites 3 and 4 are characterized by a rebonding, leaving Sb 3-fold coordinated and sticking out of the surface. These new “pushed-up” reconstructions are more stable (lower in energy) by an average of 0.5 eV (0.75 eV) for Sb (Bi) compared to a substitutional placement in the original Pandey model, which was found to represent only a local energy minimum. The simulated STM images of all ground state reconstructions were furthermore found to give a satisfactory match with the measured topography images. There is excellent agreement for sites 1, 3, and 4, with each of these sites displaying the very distinctive features in the correct orientation. The agreement for site 2 is less striking but still reasonable, displaying the Sb atom and the two adjacent up atoms as a protrusion with the protrusion overlapping with the row above. Dark regions seen by STM on either side of site 2 and site 3, which are long-range electrostatic effects, are not expected to be reproduced in DFT because the simulation cell would need to be significantly longer than the dark regions.

This result not only confirms that the measured features represent Sb and Bi atoms in the four substitutional surface sites but also highlights the influence of the different group V elements. Since P in the Si(111)2 × 1 has been shown to sit in the substitutional sites of the original Pandey reconstruction,<sup>19</sup> it is assumed that the “pushed-up” reconstructions for Sb and Bi are induced by inherent properties of the atomic element such as electronic potential or size.<sup>20</sup> To determine the influence of the different atomic elements we have calculated the energy gained by forming the new reconstruction for all group V atoms as shown in Table 1. It can be seen that for all three sites the energy gain increases when moving down in the

periodic table, indicating that the size of the atom plays a significant role in determining its reconstruction, in good agreement with the fact that we observed the two largest atoms, Sb and Bi, in the “pushed-up” state, whereas P, the smallest element, was observed in the Pandey reconstruction.<sup>19</sup> However, it is interesting to note that DFT calculations still predict an energy gain when forming the “pushed-up” reconstruction for P, in disagreement with previous experimental observations.<sup>19</sup> Doubling the cell size to increase the distance between two dopants across the  $\pi$ -bonded chains changes the total energy differences between a site 3 Pandey and site 3 pushed-up structures by 0.02 eV, an insignificant amount. Similar magnitude corrections to the energy differences are expected to be found for the other structures. Since P was measured at 8 K, the difference in measurement temperatures might further contribute to the observed discrepancies, given that the one-dimensional conduction of  $\pi$ -bonded chains has been shown to be strongly temperature dependent.<sup>18</sup> It is noted at this point that, similar to P, a sixth feature was found exclusively on the Sb wafer which could not be assigned to the Sb atoms (see Supporting Information, Figure S2).

The newly identified, pushed-up reconstructions can additionally be used to elucidate the measured site-dependent charge states if considered in conjunction with the delicate interplay of structure and charge in the Si(111) $2 \times 1$  reconstruction.<sup>21</sup> As shown in Figure 3a, an electron transferred from the  $sp^2$  hybridized “down” buckled atom to the  $sp^3$  hybridized “up” buckled atom creates positively and negatively charged silicon atoms, respectively, within the  $\pi$ -bonded chain. When evaluating charge states on the surface it is therefore crucial to not only consider the group V atom itself but also how it influences the charge distribution on surrounding atoms and whether it substitutes a positively charged up atom or a negatively charged down atom. To do so, charge states of all surface atoms were extracted from DFT calculations, based on bond angles indicating  $sp^2$  or  $sp^3$  hybridization, as described in Supporting Information, Figure S3. Results are shown in Figure 3b–e for the example of Sb, whereas identical results were obtained for Bi. It can be seen that the Sb atoms themselves always retain a filled lone pair in all four surface sites, corresponding to five valence electrons and therefore to an electrically neutral state, seemingly in contradiction to the measured charges shown in Figure 3c. However, if surrounding atoms are taken into account as well, we found that the total charge on the surface is in excellent agreement with the measurement.

In Figure 3b it can be seen that for site 1 the neutral Sb atom replaces the negatively charged Si up atom while its associated down atoms retain an empty lone pair and therefore a positive charge state. The fact that atoms surrounding the Sb atom retain the same charge state as in the native surface reconstruction disturbs

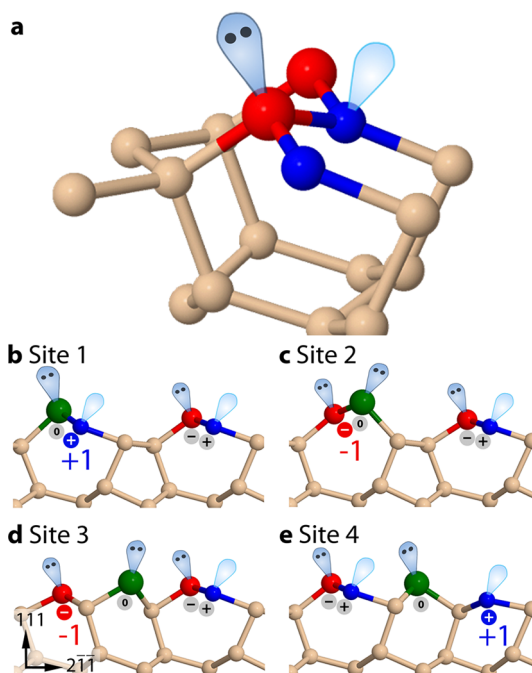


**Figure 3.** (a) Charge distribution on the clean Si(111) $2 \times 1$  surface. (b–e) Charge distribution of the ground state reconstructions for site 1–4 extracted from DFT calculations. The atoms colored red, blue, and green represent up-buckled Si, down-buckled Si, and substituted Sb atoms, respectively.

the charge balance, and an uncompensated positive charge located on the down atoms remains, in excellent agreement with the measurement. A similar mechanism creates the negative charge state for site 2, where the neutral Sb replaces the positively charged silicon down atom, leading to an uncompensated negative charge, located on the adjacent Si up atoms. For site 3 on the other hand, the neutral Sb is replacing a 4-fold coordinated, neutral silicon atom and is therefore not directly changing the surface charge balance. However, because of the newly induced pushed-up reconstruction, the down atom to the left of the Sb is rebonded and becomes 4-fold coordinated and therefore electrically neutral. The new reconstruction thus disturbs the charge balance and creates a negative charge, located on the remaining up atoms in the  $\pi$ -bonded chain to the left of the Sb atom. For site 4 a similar process occurs, where the negatively charged up atom to the right of the Sb is rebonded and creates a positive charge, located on the remaining down atoms in the  $\pi$ -bonded chain to the right of the Sb, in excellent agreement with the measurement. The observed charge states are therefore not caused by an ionization of group V atoms in the surface but are a result of the newly induced reconstructions which are a trapping charge in a location laterally displaced from the group V atoms.

To confirm the predicted position of the charge, Sb3 is shown in Figure 4a,b measured at 1.1 and 0.5 V, imaging predominantly bulk and surface states, respectively.<sup>13,22</sup> It can be seen that the circular depression measured at

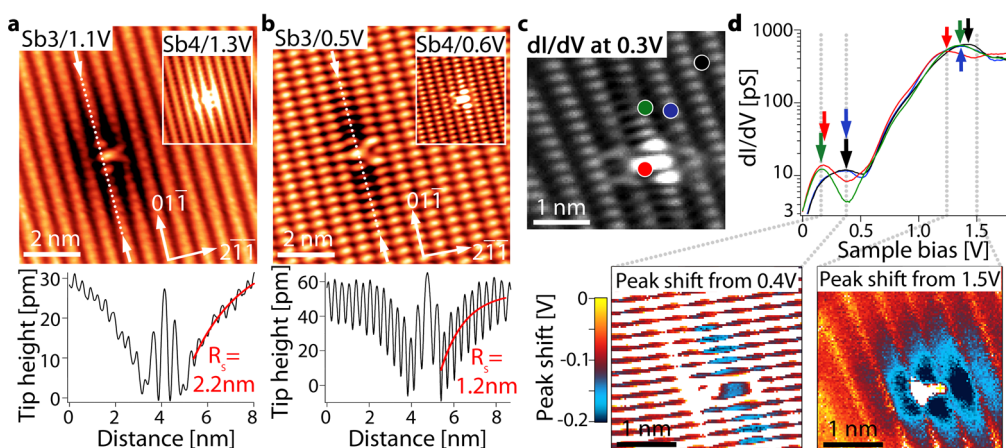


**Figure 4.** (a,b) (Top) Topography image of Sb3 (Sb4 inset) measuring predominantly bulk and surface states, respectively. (Bottom) Screening lengths extracted from cross-sectional height profiles as indicated by the dotted line. (c)  $dI/dV$  map of Sb4, extracted from a CITS measurement. (d) STS extracted from four different locations of a CITS scan of Sb4, as indicated in panel c. The laterally resolved shift of the surface peak (0.5 V) is plotted below left and is confined to the direction of the  $\pi$ -bonded chains, whereas the shift in the bulk states (1.2 V), plotted below right, decays radially.

1.1 V, associated with the screened coulomb potential of the charge,<sup>12</sup> becomes strongly confined to the direction of the  $\pi$ -bonded chains when imaged at 0.5 V, presumably reflecting the strongly asymmetric screening of the charge in the surface band. The same behavior was observed for all Bi and Sb atoms, with the positively charged reconstructions displaying protrusions rather than depressions, as can be seen in the inset for Sb4, similar to previous observations for P and boron (B).<sup>17,23</sup> The fact that the depression for Sb3 is located in the  $\pi$ -bonded chain to the left of the Sb atom, whereas the protrusion of Sb4 is located in the  $\pi$ -bonded chain to the right of the Sb atom excellently matches the position of the charge as shown in Figure 3, in strong agreement with the DFT model.

Whereas the observed confinement of the charge to the direction of the  $\pi$ -bonded chains is in good agreement with theoretical predictions,<sup>24</sup> the exact shape of the screened potential well is still a subject of current debate, depending strongly on the degree to which electrons have been confined to a single  $\pi$ -bonded chain.<sup>24–26</sup> A current imaging tunnelling spectroscopy (CITS) map of Sb4 was acquired, shown in Figure 4c, and STS curves extracted at different locations are shown in Figure 4d. It can be seen that band bending is not rigid,<sup>27</sup> as the surface state peak (0.4 V) is shifted only within the  $\pi$ -bonded chain containing the charge, whereas the shift of the bulk peak (1.1 V) decays radially with increasing distance from the Sb atom. By plotting the lateral dependence of the shift in the two peaks individually we are able to use the high

lateral and energetic resolution of STS to map out the potential well in surface and bulk states independently, as shown in the lower part of Figure 4d. From these maps the confinement of the charge is clearly visible, showing the potential well extended along the direction of the  $\pi$ -bonded chains in the surface state, whereas it decays radially in the bulk states, in good qualitative agreement with theoretical predictions.<sup>28</sup> Screening radii were furthermore extracted from the topography images<sup>28</sup> as shown in the lower part of Figure 4a,b and were found to be 1.2 nm in the surface and 2.2 nm in the bulk states, a ratio close to the theoretically predicted value of 2.<sup>24</sup>

## CONCLUSIONS

In this work we have characterized solitary Bi and Sb atoms in silicon at the atomic scale, demonstrating how they induce ambipolar charge states depending on their crystal site and their element-dependent atomic reconstruction. The ability of Sb and Bi to induce ambipolar charge in their vicinity is striking and provides interesting possibilities for the design of future atomic-scale devices, possibly improving scattering characteristics<sup>29</sup> and modifying hyperfine interactions with the nucleus. Furthermore we were able to map the spatial extent of the potential well of these charges in different electronic bands, providing vital insights into fundamental mechanisms of charge screening near interfaces. These findings demonstrate how characteristics of group V atoms are crucially altered in surfaces or interfaces and further highlight important implications for the choice of donor element, the design, and the fabrication methods of future atomic-scale devices.

## METHODS

Experiments were performed at 78 K in an Omicron LT-STM with a base pressure below  $5 \times 10^{-11}$  mbar. To expose an atomically flat Si(111) surface, samples were cut from a Si(211)

wafer, cleaved *in situ* at room temperature and subsequently loaded into the precooled STM. This surface preparation method does not include any thermal annealing steps after cleaving and is therefore ideally suited to characterize dopants in

intrinsic silicon crystal positions. Sb atoms were measured on a bulk doped wafer purchased from NOVA Semiconductors with a conductivity smaller than  $0.02 \Omega\text{cm}$ , corresponding to a doping level higher than  $1 \times 10^{18} \text{ cm}^{-3}$ . Bi atoms on the other hand are, due to their low equilibrium solid solubility limit, not commercially available in high bulk doped silicon wafers. Samples were therefore prepared using ion implantation and subsequent annealing, resulting in an electrically active Bi concentration of  $7 \times 10^{18} \text{ cm}^{-3}$ , as described in the Supporting Information. The results described in this paper were reproducible with a number of STM tips; 2 for Sb and 5 for Bi, and on a similar number of samples. All tips were made of tungsten wire and prepared using electrochemical etching in a KOH solution. Once in UHV the tips were treated using electron beam heating and field emission, such that they gave reproducible atomic resolution images and  $I-V$  spectra.

Bi and Sb atoms were identified by characterizing all repeatedly occurring features on the surface as shown in Figure 1c. For the Sb-doped wafer, 99 features were measured, corresponding to a density of  $2 \times 10^{18} \text{ cm}^{-3}$  within the investigated area, in excellent agreement with the expected doping density of the sample. For the Bi implanted wafer, significant parts of the surface were disturbed by remaining implantation damage and estimating the average dopant concentration was therefore not possible. However, samples were characterized before and after implantation and all observed features were found exclusively in the implanted samples, correlating them directly to the process of Bi dopant implantation.

DFT calculations were performed using VASP<sup>30</sup> with the PBE<sup>31</sup> functional. As described in more detail in the Supporting Information, a 10-layer Si slab (320 atoms), with the top 8 layers free to move and the bottom terminated with H (32 atoms) was used.

**Conflict of Interest:** The authors declare no competing financial interest.

**Acknowledgment.** The authors thank F. Giebl and A. Fisher for stimulating discussions. The calculations were done at the University College London High Performance Computing cluster and at the UCL London Centre for Nanotechnology HPC service. Ion implantation of Bi was performed at the University of Surrey Ion Beam Centre. This work was supported by the Engineering and Physical Sciences Research Council (EPSRC) through grants EP/H026622/1 and EP/D063329/1. S.R.S. acknowledges EP/H003991/1 (Career Acceleration Fellowship) and P.S. acknowledges EP/J500331/1 (EPSRC Doctoral Prize).

**Supporting Information Available:** Additional supporting STM figures of all Bi and Sb dopants as well as detailed information about experimental procedures and DFT simulations. This material is available free of charge via the Internet at <http://pubs.acs.org>.

## REFERENCES AND NOTES

- Fuechsle, M.; Miwa, J. A.; Mahapatra, S.; Ryu, H.; Lee, S.; Warschkow, O.; Hollenberg, L. C.; Klimeck, G.; Simmons, M. Y. A Single-Atom Transistor. *Nat. Nanotechnol.* **2012**, *7*, 242–246.
- Koenraad, P. M.; Flatte, M. E. Single Dopants in Semiconductors. *Nat. Mater.* **2011**, *10*, 91–100.
- Morton, J. J.; McCamey, D. R.; Eriksson, M. A.; Lyon, S. A. Embracing the Quantum Limit in Silicon Computing. *Nature* **2011**, *479*, 345–53.
- Stoneham, A. M.; Fisher, A. J.; Greenland, P. T. Optically Driven Silicon-Based Quantum Gates with Potential for High-Temperature Operation. *J. Phys.: Condens. Matter* **2003**, *15*, L447–L451.
- Morley, G. W.; Warner, M.; Stoneham, A. M.; Greenland, P. T.; van Tol, J.; Kay, C. W. M.; Aeppli, G. The Initialization and Manipulation of Quantum Information Stored in Silicon by Bismuth Dopants. *Nat. Mater.* **2010**, *9*, 725–729.
- Benjamin, S. C. Quantum Computing without Local Control of Qubit–Qubit Interactions. *Phys. Rev. Lett.* **2001**, *88*, 017904.
- de Sousa, R.; Lo, C. C.; Bokor, J. Spin-Dependent Scattering in a Silicon Transistor. *Phys. Rev. B* **2009**, *80*, 045320–9.
- Rockett, A.; Johnson, D. D.; Khare, S. V.; Tuttle, B. R. Prediction of Dopant Ionization Energies in Silicon: The Importance of Strain. *Phys. Rev. B* **2003**, *68*, 233208.
- Picraux, S. T.; Brown, W. L.; Gibson, W. M. Lattice Location by Channeling Angular Distributions: Bi Implanted in Si. *Phys. Rev. B* **1972**, *6*, 1382.
- Pandey, K. C. New  $\pi$ -Bonded Chain Model for Si(111)-(2 × 1) Surface. *Phys. Rev. Lett.* **1981**, *47*, 1913.
- Lequn, L.; Jixin, Y.; Lyding, J. W. Subsurface Dopant-Induced Features on the Si(100)2 × 1:H Surface: Fundamental Study and Applications. *IEEE Trans. Nanotechnol.* **2002**, *1*, 176–183.
- Ebert, P. Defects in III–V Semiconductor Surfaces. *Appl. Phys. A: Mater* **2002**, *75*, 101–112.
- Garleff, J. K.; Wenderoth, M.; Sauthoff, K.; Ulbrich, R. G.; Rohlfing, M. 2 × 1 Reconstructed Si(111) Surface: STM Experiments versus *ab Initio* Calculations. *Phys. Rev. B* **2004**, *70*, 245424.
- Himpsel, F. J.; Hollinger, G.; Pollak, R. A. Determination of the Fermi-Level Pinning Position at Si(111) Surfaces. *Phys. Rev. B* **1983**, *28*, 7014.
- Radny, M. W.; Smith, P. V.; Reusch, T. C. G.; Warschkow, O.; Marks, N. A.; Wilson, H. F.; Curson, N. J.; Schofield, S. R.; McKenzie, D. R.; Simmons, M. Y. Importance of Charging in Atomic Resolution Scanning Tunneling Microscopy: Study of a Single Phosphorus Atom in a Si(001) Surface. *Phys. Rev. B* **2006**, *74*, 113311.
- Garleff, J.; Wijnheijmer, A.; v. d. Enden, C.; Koenraad, P. Bistable Behavior of Silicon Atoms in the (110) Surface of Gallium Arsenide. *Phys. Rev. B* **2011**, *84*, 075459.
- Trappmann, T.; Suergers, C.; Loehneysen, v. Observation of P Donors on the Si(111) Surface by Scanning Tunneling Microscopy. *Europhys. Lett.* **1997**, *38*, 177.
- Garleff, J. K.; Wenderoth, M.; Ulbrich, R. G.; Suergers, C.; Loehneysen, H. v. Evidence for One-Dimensional Electron Propagation on Si (111)-(2 × 1) from Coulomb Blockade. *Phys. Rev. B* **2005**, *72*, 073406.
- Garleff, J. K.; Wenderoth, M.; Ulbrich, R. G.; Suergers, C.; v. Lohneysen, H.; Rohlfing, M. Identification of P Dopants at Nonequivalent Lattice Sites of the Si(111)-(2 × 1) Surface. *Phys. Rev. B* **2007**, *76*, 125322–5.
- Pajot, B.; Stoneham, A. M. A Spectroscopic Investigation of the Lattice Distortion at Substitutional Sites for Groups V and VI Donors in Silicon. *J. Phys. C* **1987**, *20*, 5241.
- Rohlfing, M.; Pollmann, J. Localization of Optically Excited States by Self-Trapping. *Phys. Rev. Lett.* **2002**, *88*, 176801.
- Stroscio, J. A.; Feenstra, R. M.; Fein, A. P. Electronic Structure of the Si(111)2 × 1 Surface by Scanning-Tunneling Microscopy. *Phys. Rev. Lett.* **1986**, *57*, 2579–2582.
- Schock, M.; Suergers, C.; Von Lohneysen, H. Investigation of Single Boron Acceptors at the Cleaved Si: B(111) Surface. *Phys. Rev. B* **2000**, *61*, 7622–7627.
- Reining, L.; Del Sole, R. Screened Coulomb Interaction at Si(111)2 × 1. *Phys. Rev. B* **1991**, *44*, 12918.
- Reining, L.; Del Sole, R. Quasi One Dimensional Excitons and the Optical Properties of Si(111)2 × 1. *Phys. Rev. Lett.* **1991**, *67*, 3816.
- Rohlfing, M.; Louie, S. G. Excitons and Optical Spectrum of the Si(111)2 × 1 Surface. *Phys. Rev. Lett.* **1999**, *83*, 856.
- Lee, D. H.; Gupta, J. A. Tunable Field-Control over the Binding Energy of Single Dopants by a Charged Vacancy in GaAs. *Science* **2010**, *330*, 1807–1810.
- Hamers, R. J. Characterization of Localized Atomic Surface Defects by Tunneling Microscopy and Spectroscopy. *J. Vac. Sci. Technol. B* **1988**, *6*, 1462–1467.
- Dingle, R.; Stormer, H. L.; Gossard, A. C.; Wiegmann, W. Electron Mobilities in Modulation-Doped Semiconductor Heterojunction Superlattices. *Appl. Phys. Lett.* **1978**, *33*, 665–667.

30. Kresse, G.; Furthmüller, J. Efficiency of Ab-Initio Total Energy Calculations for Metals and Semiconductors Using a Plane-Wave Basis Set. *Comput. Mater. Sci.* **1996**, *6*, 15–50.
31. Perdew, J. P.; Burke, K.; Ernzerhof, M. Generalized Gradient Approximation Made Simple. *Phys. Rev. Lett.* **1996**, *77*, 3865–3868.